

## A Gamma-Spectrometer Ground Installation for Detecting Cosmic Rays in the Casleo Astronomic Complex

M. V. Philippov<sup>a,\*</sup>, V. S. Makhmutov<sup>a</sup>, A. N. Kvashnin<sup>a</sup>, O. S. Maksumov<sup>a</sup>,  
Yu. I. Stozhkov<sup>a</sup>, J.-P. Raulin<sup>b</sup>, and J. Tacza<sup>b</sup>

<sup>a</sup> Lebedev Physical Institute, Russian Academy of Sciences,  
Moscow, 119991 Russia

<sup>b</sup> Universidade Presbiteriana Mackenzie, EE, CRAAM, Sao Paulo, Brazil  
\*e-mail: mfilippov@frtk.ru

Received January 21, 2021; revised February 4, 2021; accepted February 6, 2021

**Abstract**—The description and technical characteristics of the gamma-spectrometer installation for the detection of cosmic rays, as designed at the Dolgoprudny scientific station of the Lebedev Physical Institute in cooperation with the Mackenzie University (Sao Paulo, Brazil), are presented. This installation has operated continuously in the CASLEO astronomical complex since 2015. The detector modules of the setup are based on the NaJ (Tl) scintillator, which is 76.2 mm × 76.2 mm high, a Hamamatsu R1307 photomultiplier tube, a high voltage power supply, and a preamplifier. The technique of the experimental calibration of the spectrometer is also presented.

DOI: 10.1134/S0020441221040035

### INTRODUCTION

The hardware–software complex of a Gamma-spectrometer was developed in 2014 at the Dolgoprudnenskaya Scientific Station (DNS) of the Lebedev Physical Institute within the framework of international cooperation with scientists from Brazil and Argentina, which is designed to detect and determine the energy spectra of secondary  $\gamma$ -quants [1]. This equipment is installed at the CASLEO observatory (Argentina, S31.47°, W69.17°, at an altitude of 2550 m above sea level and a geomagnetic cutoff rigidity of  $R_c = 9.8$  GV), where the complex of cosmic ray detectors that was previously developed at the FIAN DNS is currently operating. CARPET, the first facility that records the charged component of cosmic rays, was launched in 2006 [2–7]. In 2015, the Gamma-spectrometer and the neutron detector device for recording the neutron component of cosmic rays were launched [8, 9].

This paper presents the circuitry solutions used in the development of the Gamma-spectrometer and its characteristics. The background radiation calibration technique is also presented.

### THE HARDWARE AND SOFTWARE COMPLEX

The Gamma-spectrometer contains four detecting modules (Fig. 1), which are based on the 12S12/3.VD.HVG.PA scintillation assembly manu-

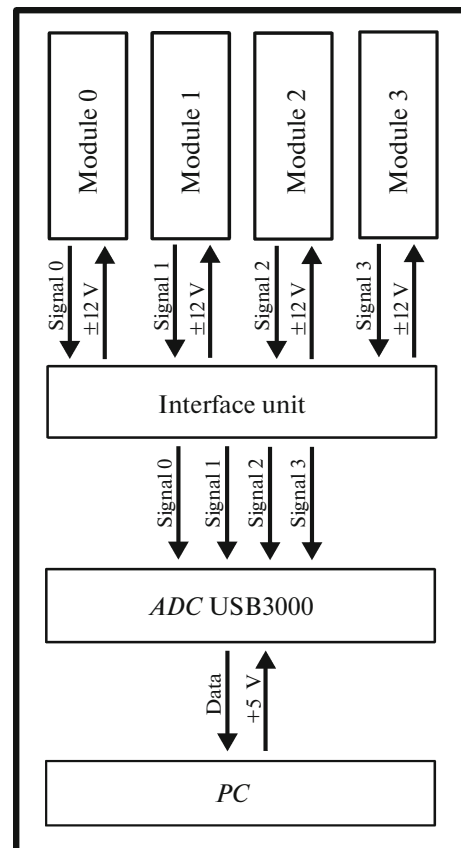


Fig. 1. A block diagram of the Gamma-spectrometer. ADC, analog-to-digital converter; PC, personal computer.

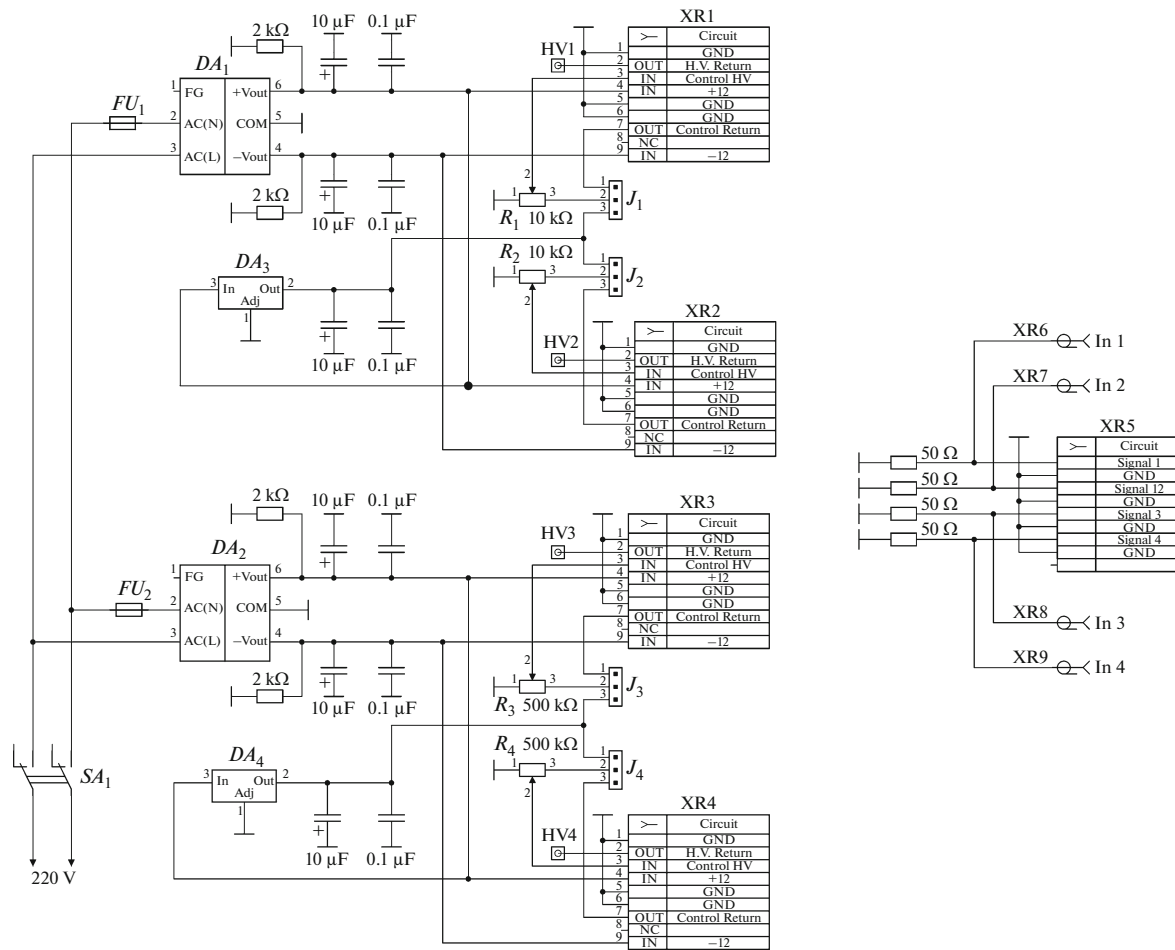


Fig. 2. A schematic diagram of the gamma-spectrometer interface module.  $DA_1, DA_2$ —TML05212;  $DA_3, DA_4$ —LM1117-5.0.

factured by ScintiTech (<http://www.scintitech.com/>). The scintillation assembly includes a Hamamatsu R1307 photomultiplier tube (PMT) (<https://www.hamamatsu.com/jp/en/product/type/R1307/index.html>) 76 mm in diameter, an NaI (TI) scintillator with a height of 76.2 mm and an electronic unit, which consists of a high-voltage converter, a voltage divider and a preamplifier. A voltage of  $\pm 12$  V is required to power the electronic unit.

The interface unit we developed (Fig. 2) is designed to connect four detecting modules via power connectors (XR1–XR4) and signal connectors (XR6–XR9). Primary supply voltages  $\pm 12$  V are generated on TML 05212 converters ( $DA_1$  and  $DA_2$ ). Each transducer supplies two detection modules. The output voltages of the high-voltage converters of the scintillation assemblies are adjustable in the range from  $-200$  V to  $-1500$  V, which makes it possible to set a high voltage for each PMT individually using potentiometers  $R_1$ – $R_4$ .

Using the XR5 connector, signals from the detection modules are fed to an analog-to-digital converter (ADC) USB3000 (<http://www.r-technology.ru/products/adc/usb3000.php>), where they are converted to a

sequence of two-byte samples. Each count is a number in the range from  $-8000$  to  $+8000$  (maximum amplitude resolution), which corresponds to the signal range from  $-5$  to  $+5$  V. Since the signals from the detecting modules are positive, the output ADC a sequence of samples is obtained in the range from 0 to 8000. Therefore, the signal quantization step is  $-625$   $\mu$ V.

Data transfer from ADC to PC is carried out via the USB bus. In the software settings one can set the ADC sampling rate (time resolution), the step of signal quantization by amplitude (number of channels), and the duration of the data accumulation time for each file.

The software of the PC sequentially generates files containing data received during a specified time interval (duration). Under the current conditions of the experiment, measurements are carried out with a specified duration of data files of 600 s and a sampling rate of 500 kHz, with an energy resolution of 128 channels.

Each data file in the header contains information about the start time (UTC), the sampling rate ADC and the duration of the data collection interval. Next, a table is written, which indicates the number of the energy channel, the number of pulses ( $\gamma$ -quants) that

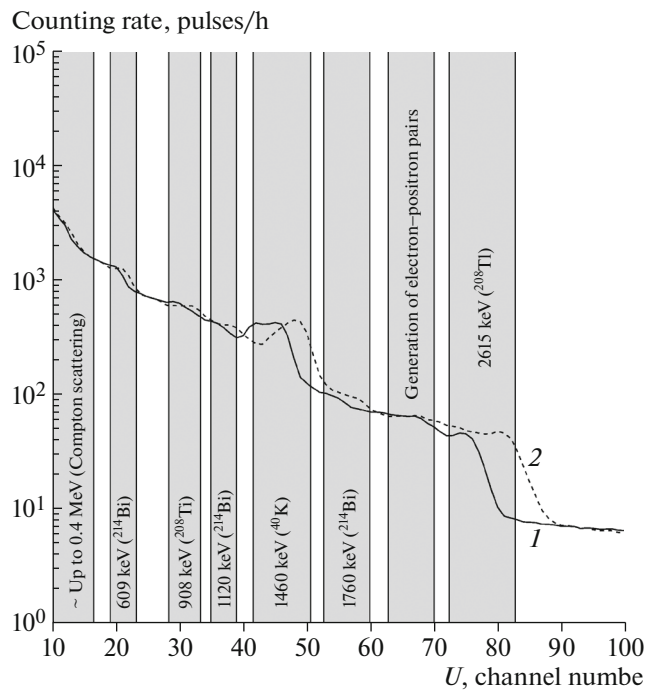


**Fig. 3.** Graphs of the differential spectrum of the module 0 Gamma-spectrometer: 1, according to data for January 2020 (summer period), 2, for June 2020 (the winter period).

entered the channel with the number  $N$  (differential spectrum), the total number  $\gamma$ -quanta that entered the channels starting from the number  $N + 1$  and higher (integral spectrum), and the  $\gamma$ -quant energy corresponding to the channel number, as calculated by preliminary calibration with  $^{60}\text{Co}$  and  $^{137}\text{Cs}$  sources.

### SPECTROMETER CALIBRATION

The detecting modules of the Gamma-spectrometer were pre-calibrated at the LPI using sources  $^{60}\text{Co}$   $\gamma$ -radiation (1.17 and 1.33 MeV) and  $^{137}\text{Cs}$  (661.7 keV). Initial calibration was necessary in order to correctly select the output voltages of the high-voltage converters: 775 V for module 0, 789 V for module 1, and 728 V for modules 2 and 3, which roughly set the ranges of the detected  $\gamma$ -quanta energies of 50 keV–3.5 MeV for modules 0 and 1 and 50 keV–5 MeV for modules 2 and 3. However, this calibration cannot be considered final, since it was carried out in laboratory conditions and does not take the instrumental effect into account, that is, the effect of temperature on the output voltage of high-voltage converters.

To illustrate the temperature effect, Fig. 3 shows the graphs of two differential spectra for the detecting module 0: spectrum 1, obtained by superimposing epochs of all 10-min spectra for January 2020, spectrum 2, as of June 2020

It was necessary to develop a method for continuous calibration of the spectrometer according to the

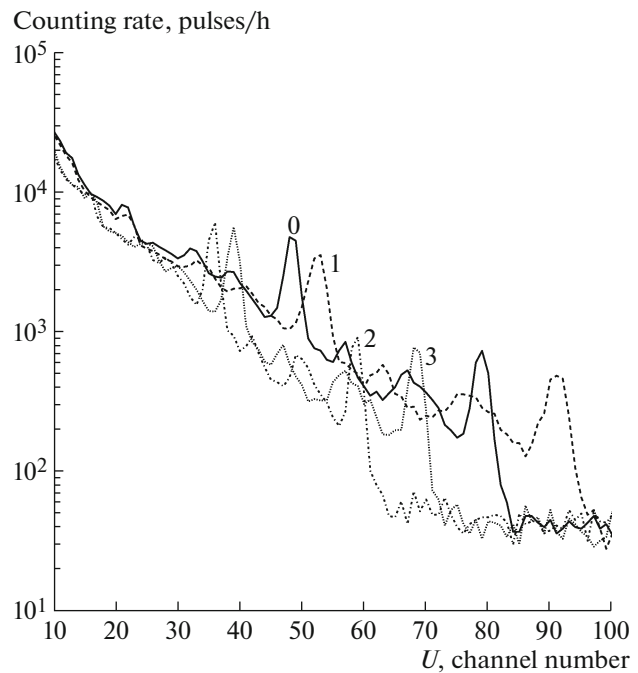


**Fig. 4.** The initial differential spectra for four detecting modules (0–3) according to the data for January 1, 2018 from 01:00 to 02:00 UTC. The numbers at the spectra correspond to the modules.

available data, which takes the temperature effect into account and does not require additional devices, since the installation operates in an autonomous mode. For calibration, one can use the spectral lines of radioactive substances in soil. The isotopes  $^{40}\text{K}$ ,  $^{214}\text{Bi}$ ,  $^{208}\text{Tl}$  were used as calibration sources for  $\gamma$ -radiation [10]. Figure 3 shows the approximate neighborhoods of the spectral lines of these isotopes. Compton scattering of energetic  $\gamma$ -quant, therefore it is not used during calibration in the energy range of  $\sim 0$ –0.4 MeV. The penultimate energy peak, which lies in the range of approximately the (65–75)th channels is a consequence of the formation of electron–positron pairs and is also not taken into account [11].

The graphs in Fig. 3 show the discrepancy between the lines of isotopes in the spectrum, which increases with increasing energy (channel number).

The initial condition is added to the existing six spectral lines:  $E(U) = 0$  at  $U = 0$ . The result is seven known points  $E_n$ :  $E_0(U_0 = 0)$ ,  $E_1(U_1)$ , ...,  $E_6(U_6)$ , dividing the entire spectral range of the detecting module into six intervals, the energy values within which we will fill with a piecewise linear function:

$$E(U) = E_n + k_n(U - U_n), \quad (1)$$

where  $E(U)$  is the energy value corresponding to the channel number  $U$ ;  $E_n$  is the initial energy value in this interval, corresponding to the channel number  $U_n$ ; and  $k_n$  is the slope coefficient of the given interpolation line:

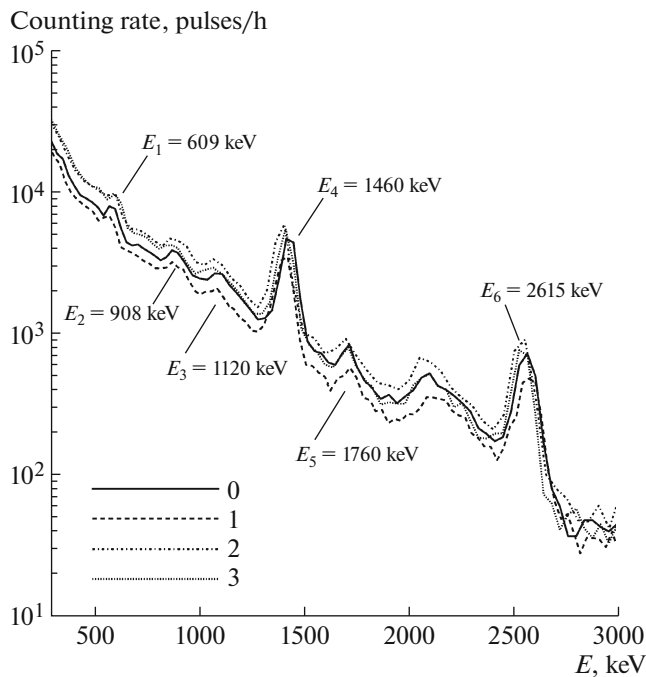


**Fig. 5.** The differential spectra for four detecting modules (0–3), after energy recalculation of  $\gamma$ -quanta, according to data for January 1, 2018 from 01:00 to 02:00 UTC.

$$k_n = \frac{E_{n+1} - E_n}{U_{n+1} - U_n}, \quad (2)$$

where  $E_{n+1}$  is the final energy value in this interval, corresponding to the channel number  $U_{n+1}$ .

To demonstrate the technique, we consider an arbitrary time interval, for example, January 1, 2018 from 01:00 to 02:00 UTC (Fig. 4). According to the most prominent peaks corresponding to  $^{40}\text{K}$ , it is clearly seen that the sensitivity of detecting modules 0 and 1 is higher than the sensitivity of detecting modules 2 and 3, due to the higher voltages set across the PMT.

Using this technique, the spectra obtained by the detecting modules were divided into six intervals, in each of which the energy values were obtained using formulas (1) and (2)  $\gamma$ -quanta depending on the channel number (Fig. 5). In the graphs in Fig. 5 some difference in the absolute values of the counting rates of the detecting modules is noticeable, which, if necessary, can be eliminated by mutual normalization according to the data of simultaneous measurements.

## CONCLUSIONS

This paper presented a description and the schematic implementation of an installation for detecting flows. The  $\gamma$ -radiation spectrometer has been continuously functioning in the CASLEO astronomical complex from 2015 to the present. For a comprehensive analysis of the experimental data, a technique has

been developed for the calibration and recalculation of the measured values of the channel numbers of the analog-to-digital converter into the energy of  $\gamma$ -quanta based on natural background sources of  $\gamma$ -radiation.

This setup is of particular interest for the study of generation processes of  $\gamma$ -radiation in thunderclouds and from lightning discharges (so-called TGF- and TLE-events) [12].

## REFERENCES

1. Murzin, V.S., *Astrofizika kosmicheskikh luchej. Uchebnoe posobie dlya vuzov* (Cosmic-Ray Astrophysics. Student's Book for Institutions of Higher Education), Moscow: Logos, 2007.
2. Makhmutov, V., Raulin, J.-P., De Mendonca, R.R.S., Bazilevskaya, G.A., Correia, E., Kaufmann, P., Marun, A., Fernandes, G., and Echer, E., *J. Phys.: Conf. Ser.*, 2013, vol. 409, no. 1, p. 012185. <https://doi.org/10.1088/1742-6596/409/1/012185>
3. Makhmutov, V.S., Stozhkov, Y.I., Raulin, J.-P., Philippov, M.V., Bazilevskaya, G.A., Kvashnin, A.N., Tacza, J., Marun, A., Fernandez, G., Viktorov, S.V., and Panov, V.M., *Bull. Russ. Acad. Sci.: Phys.*, 2017, vol. 81, no. 2, p. 241. <https://doi.org/10.3103/S1062873817020265>
4. Mizin, S.V., Makhmutov, V.S., Maksumov, O.S., and Kvashnin, A.N., *Bull. Lebedev Phys. Inst.*, 2011, vol. 38, no. 2, p. 34. <https://doi.org/10.3103/S1068335611020023>.
5. De Mendonca, R., Raulin, J.-P., Bertoni, F., Echer, E., Makhmutov, V., and Fernandes, G., *J. Atmos. Sol.-Terr. Phys.*, 2011, vol. 73, p. 1410. <https://doi.org/10.1016/j.jastp.2010.09.034>
6. De Mendonca, R.R.S., Raulin, J.-P., Echer, E., Makhmutov, V.S., and Fernandez, G., *J. Geophys. Res.: Space Phys.*, 2013, vol. 118, no. 4, p. 1403. <https://doi.org/10.1029/2012JA018026>
7. Philippov, M.V., Makhmutov, V.S., Stozhkov, Yu.I., and Maksumov, O.S., *Instrum. Exp. Tech.*, 2020, vol. 63, no. 3, pp. 388–395. <https://doi.org/10.1134/S0020441220030033>
8. Philippov, M.V., Makhmutov, V.S., Stozhkov, Y.I., Raulin, J.-P., and Kalinin, E.V., *Bull. Russ. Acad. Sci.: Phys.*, 2019, vol. 83, no. 5, p. 611. <https://doi.org/10.3103/S1062873819050137>
9. Philippov, M.V., Makhmutov, V.S., Stozhkov, Yu.I., Maksumov, O.S., Raulin, J.-P., and Tacza, J., *Instrum. Exp. Tech.*, 2020, vol. 63, no. 5, pp. 716–723. <https://doi.org/10.1134/S0020441220050292>
10. Ford, K., Harris, J.R., Shives, R., Carson, J., and Buckle, J., *Geosci. Can.*, 2008, vol. 35, nos. 3–4, p. 109.
11. Grasty, R.L., *Geophysics and Geochemistry in the Search for Metallic Ores. Geological Survey of Canada, Economic Geology Report 31*, 1979, p. 147.
12. Torii, T., Sugita, T., Kamogawa, M., Watanabe, Y., and Kusunok, K., *Geophys. Res. Lett.*, 2011, vol. 38, p. L24801. <https://doi.org/10.1029/2011GL049731>